Research Inventy: International Journal of Engineering And Science
Vol.10, Issue 12 (December 2020), PP 18-27
Issn (e): 2278-4721, Issn (p):2319-6483, www.researchinventy.com

Synthesis, Structure Determination and Study the Electrical Properties of A Novel mixed Valence of $Bi_{2.5}$ $Co_{0.25}$ $La_{1.75}$ $N_{0.21}$ Cl_5 $O_{0.25}$ Chloro Oxide by AB Initio Methods via Powder XRD

[1]Janak Adhikari,[2]Hareram Mishra,[1]Yubraj Sahu ,[1]Rohit K.Dev ,[1]Kalpana Mishra and Parashuram Mishra*
Bioinorganic and Materials Chemistry Research Lab. Tribhuvan University M.M.A.M.Campus, Biratnagar, Nepal

Abstract
The present work deals with the ab initio structure determination of the heavy metal framework $Bi_{2.5}$ $Co_{0.25}$ $La_{1.75}$ $N_{0.21}$ $O_{0.25}$ Cl_5 *from precession electron diffraction intensities The metal framework of the compound was solved in this investigation via direct methods from hk0 precession electron diffraction intensities recorded with a Philips EM400 at 100 kV. A subsequent (kinematical) least-squares refinement with electron intensities yielded slightly improved co-ordinates for the 10 heavy atoms in the structure. Chemical analysis of several crystallites by EDX is in agreement with the formula* $Bi_{2.5}$ $Co_{0.25}$ $La_{1.75}$ $N_{0.21}$ $O_{0.25}$ Cl_5 *. Moreover, the structure was independently determined by Rietveld refinement from X-ray powder data obtained from a multi-phasic sample. The compound having orthorhombic crystal system space group P-1 with refined lattice parameters a=4.214(7) Å b=7.593(11) Å c=13.051(18) Å α=82.22(8)° β=89.97(6)° γ=77.09(8)° and v=03.1 Å$^{3.}$ Comparison of the framework structure from electron diffraction with the result from Rietveld refinement shows an average agreement for the heavy atoms within 0.09A ˚ . The titled compound was prepared from mixture of* $La_2(CO_3)_3$, $Zr(NO)_2$,and$CdSO_4$ *by solid state reaction with full thermal decomposition at 1000°C. Rwp = 0.57.15, Rp = 0.5068 and GOF=0.00178 The structure factors F0 = 3032 and Fc = 3031. The morphology of the crystal has been determined by SEM and electro properties are calculated using Dilatometer.*

Key-words: *Triclinic, crystal system, determination, structure, morphology, XRD, SEM*

Date of Submission: 24-11-2020 Date of Acceptance: 07-12-2020

I. INTRODUCTION

For the past decade, there has been considerable interest in layered oxides exhibiting ferroelectric, piezoelectric and other related properties due to their wide ranging application in technical devices (Park *et al* 1999). One such family of oxides is the Aurivillius type of oxides with the general formula. The extensive search for novel inorganic materials with open frameworks formed of tetrahedra and octahedra delimiting inter-layer spaces (2D), tunnels (3D) or cages (1D) where cations are housed, represent currently a field of intense activity including several disciplines: solid-state chemistry, physics, mechanics, and mainly ionic conductivity properties and their use as battery materials. Metal oxide compounds containing lanthanide elements have greatly attract significant interest for their technologically important applications in many different fields, such as laser pumping, frequency conversion, photo luminescence, magnetic materials, and scintillator crystals.[1] In order to explore new materials with unique performances, oxo anions of group 13, 14, and 15 elements have been introduced and combined with lanthanides led to a variety of new framework materials, such as lanthanide silicates and lanthanide germanates.[2] Although both sets of compounds exhibit high thermal stability and interesting optical and magnetic properties, compared with lanthanide silicates, germanate analogs are less investigated. For the ternary lanthanide germanates, some reported compounds feature interesting properties for potential applications. For example, apatite-type La9.33Ge6O26 single crystal works as an oxide ionic conductor,[3] Ho2Ge2O7 shows significantly anisotropic magnetic properties,[4] and Eu2GeO5 exhibits strong red light emission. Ternary lanthanide germinates greatly increase the opportunities of performance modifications by introducing a more diverse set of atoms with differing radii and electronegativity. For example, La2MgGeO6 features a aurvillus structure which is very scarce in Ge based compounds. YFeGe2O7 exhibits a remarkable low-temperature ferromagnetic ordering phenomenon. Our previously work Eu2GeB2O8 shows a strong red emission. In alkali metal lanthanide germanate system, most reported compounds are based on sodium cations. Compounds with other cations are surprisingly limited. The only examples we can find in the references are LiNdGeO4 and KEuGe2O6.[5] So far, no rubidium or cesium lanthanide germanate has been reported. We deem alkali metal template cations with different radii may lead to new lanthanide germanates with different frameworks and physical properties.[6] Our research efforts in this field led to the discovery of

RbNdGe2O6Herein, we reported its synthesis, crystal structure, and physical properties, especially for its visible-light-driven photo degrade methylene blue. Phosphates of transition metals and alkaline cations are well known for their thermal stability and the simplicity of syntheses [7], which is important for many practical applications. Recently, research groups have concentrated on Na-ion batteries, as sodium is less toxic and is abundant in nature [8]. Numerous new compositions have been recently prepared and tested for electrical and/or electrochemical properties, e.g. NaCo(PO3)3 [7], Na4Ni3(PO4)2P2O7 [8], Na2Ni2Cr(PO4)3 [9], Na1.86Fe3(PO4)3 [10]. Sodium cobalt diphosphate Na2CoP2O7 is a well-known material due to its high activation energy (7.63 eV) of ionic conductivity [11] and due to its higher thermal stability compared to the other phosphate materials [12]. The sodium atoms are located in the interlayer space, which is formed by cobalt and phosphorus polyhedra [13]. This material is a good candidate as a cathode in Na-ion batteries given its crystal structure, thermal stability and presence of cobalt metal. It has been shown recently to have reversible capacity close to 80 mA h g-1 involving Co3+/Co2+ redox activity with an average potential of 5V [14]. In this work, we undertake an attempt to determine the structure of $\mathbf{Bi_{2.5}\ Co_{0.25}\ La_{1.75}\ N_{0.21}\ O_{0.25}\ Cl_5}$by ab initio methods via powder XRD.The possibility of such substitution may be expected based on the previously reported examples of mixed compositions (e.g. K3Al2As1.92P1.08O12 [14]) and isostructural phosphates and arsenates, e.g. Na4Co7-xAl0.67x (As1-yPyO4)6 (x = 1.60; y= 0.116) [15] vs. vs. Na4Co7(PO4)6 [16]. Furthermore, sodium cobalt arsenate materials show good electrical properties, e.g. NaCoAs3O10 with activation energy (Ea) of ionic conductivity of ~0.48 eV [17], and Na4Co5.63Al0.91(AsO4)6 [18] with Ea=0.53 eV.

II. MATERIALS AND METHODS

All chemicals used were analytical grade. A polycrystalline sample of $\mathbf{Bi_{2.5}\ Co_{0.25}\ La_{1.75}\ N_{0.21}\ Cl_5\ O_{0.25}}$ was synthesized by a standard solid state reaction using a mixture of high purity reagents of Bi_2O_3−La(NO3)3 and $CoCl_3$ as the starting materials in the molar ratio of 1 : 1 : 1. The mixture was ground carefully, homogenized thoroughly with methanol (99%) in an agate mortar and then packed into an alumina crucible and calcined at 1100°C in air for 10h with several intermediate grindings[6]. Finally the product was pressed into pallets and sintered at 100 K/h. Powder X-ray diffraction (XRD) data were collected at room temperature in the angular range of2 θ =5 to 90 with scan step width of 0.02° and a fixed containing time of 15 s using Philips powder diffractometer with graphite monochromatic CuKa radiation having wave length(1.545612(A). The powder was rotated during the data collection to minimize preferred Orientation effect if any. The program TREOR in CRYSFIRE was used to index the powder pattern which give orthorhombic cell system.SIRPOW92 was used to locate the positional parameters of constituent atoms. The full pattern is fitting and peak decomposition in the space group Pcnb using check cell program. The structural parameters were refined by the Reitveld method using the GSAS program which gave Rwp = 0.5068, Rp= 0.5715 GOF = 0.0178. The density is determined by Archimedes principle. For the electrical studies, the measurements were preceded by a pretreatment of thesample in order to reduce the mean particle size of the obtained powder After these treatments, the sample achieved about 85% of the theoretical density with the final diameter of 8 mm and thickness of 2 mm. The relative density of the sample before the mechanical grinding was 79 %. Platinum electrodes were connected to the two faces of the pellet via a platinum paste to keep good electric contacts. Impedance spectroscopy measurements were carried out using a Hewlett-Packard 4192a Impedance Analyzer. The impedance spectra were recorded in the 5 Hz-13 MHz frequency range. Electrical conductivity measurements of representative $\mathbf{Bi_{2.5}\ Co_{0.25}\ La_{1.75}\ N_{0.21}\ O_{0.25}\ Cl_5}$ were carried out by complex impedance spectroscopy with a 1174 Solartron frequency response analyzer coupled to a 1286 Solartron electrochemical interface. Pellets of about 14 mm diameter and 1 mm thickness were prepared by cold pressing of a mechanically activated powder mixture with the composition: $\mathbf{Bi_{2.5}\ Co_{0.25}\ La_{1.75}\ N_{0.21}\ O_{0.25}\ Cl_5}$**.To** form the phase, the pellets were heated at 1000^0C during 12 h and slowly cooled to room temperature. This synthesis method was employed to improve the ceramic quality, as it has been shown for other materials. The formed phases and crystallinity were studied by X-ray powder diffraction. Platinum electrodes were deposited on the two faces by sputtering, and measurements were carried out in the temperature range 200-6503^{o}C, at steady temperatures, with pellets under airflow the frequency range was fixed[18].

III. RESULTS AND DISCUSSIONS

The extensive search for novel inorganic materials with open frameworks formed of tetrahedral and octahedral delimiting inter-layer spaces (2D), tunnels (3D) or cages (1D) where cations are housed, represent currently a field of intense activity including several disciplines: solid-state chemistry, physics, mechanics, and mainly ionic conductivity properties and their use as battery materials oxides of metals and alkaline cations are well known for their thermal stability and the simplicity of syntheses , which is important for many practical applications. Different type batteries [19]. Recently, research groups have concentrated on Bi-ion batteries, as sodium is less toxic and is abundant in nature. This material is a good candidate as a cathode in Co-ion batteries

given its crystal structure, thermal stability and presence of cobalt metal. It has been shown recently to have reversible capacity close to 80 mA h g^{-1} involving Bi/Co redox activity with an average potential of 3V [20].

Crystal Structure of $Bi_{2.5}$ $Co_{0.25}$ $La_{1.75}$ $N_{0.21}$ O $_{0.25}$ Cl_5

The framework structure of **$Bi_{2.5}$ $Co_{0.25}$ $La_{1.75}$ $N_{0.21}$ O $_{0.25}$ Cl_5** was first examined by ab initio structure determination method using the powder XRD data. The initial lattice parameters were determined to be parameters and V=279.7571 $Å^3$. by an indexing procedure using the program TREOR15 in EXPO2004.16 The most probable space group was suggested to be P1 triclinic crystal system Next, the integrated intensities were extracted by the Le Bail method using the program Jana2006.14 A profile function and background function of the Le Bail method used in the present study were pseudo-Voigt function and 20thorder Legendre function, respectively. An initial structure model was then obtained by the charge flipping (CF) method17 using the extracted integrated intensities. Although the La and Co site could not be clearly determined by the CF method using the powder XRD data, the framework structure of **$Bi_{2.5}$ $Co_{0.25}$ $La_{1.75}$ $N_{0.21}$ O $_{0.25}$ Cl_5** was successfully determined with the help of Reitveld refinement. Rietveld refinement of Triclnic cristal system having P-1 space group was found with three dimension structure as follows against XRD data for structural determination proved difficult, due to a combination of preferred orientation of the plate-like crystallites in flat-plate geometry[21].In other words, the extracted peak intensities for multiphase 1 could be reliable. Note that if the relative intensities differed a lot from the simulated patterns of the known phases, additional manual partitioning of those overlapping peaks would be necessary to get reliable intensities for the unknown phase 1. After considering the multiplicity and Lorentz-polarization correction, the intensities of phase 1 were used for the structure solution as below. Moreover, the reflection conditions indicated possible space groups P-1 . The initial structure model was obtained using a charge flipping algorithm with the program Superflip.8 [22] Random phases were used at the beginning of the charge-flipping iteration, and overlapping peaks were re-partitioned using a histogram match to improve the convergence. The iteration converged with an R factor of 29% and the final electron density shows a P-1 symmetry with a 5% error. The program of EDMA was then used to automatically assign atomic positions shown table 2 . Four unique heavy atomic positions were found and the heaviest one was assigned as Bi while the others were considered as Mn and Mo. Due to the existence of heavy atoms, all oxygen positions were ambiguous in the electron density map of this stage[14]. To locate the oxygen atoms, a Monte-Carlo based simulated annealing process with the program TOPAS was applied. For each annealing process, various atomic coordinates were randomly assigned as the initial positions of the oxygen atoms. The annealing process was restarted after finding a few oxygen positions, until all oxygen positions were found to be reasonable.

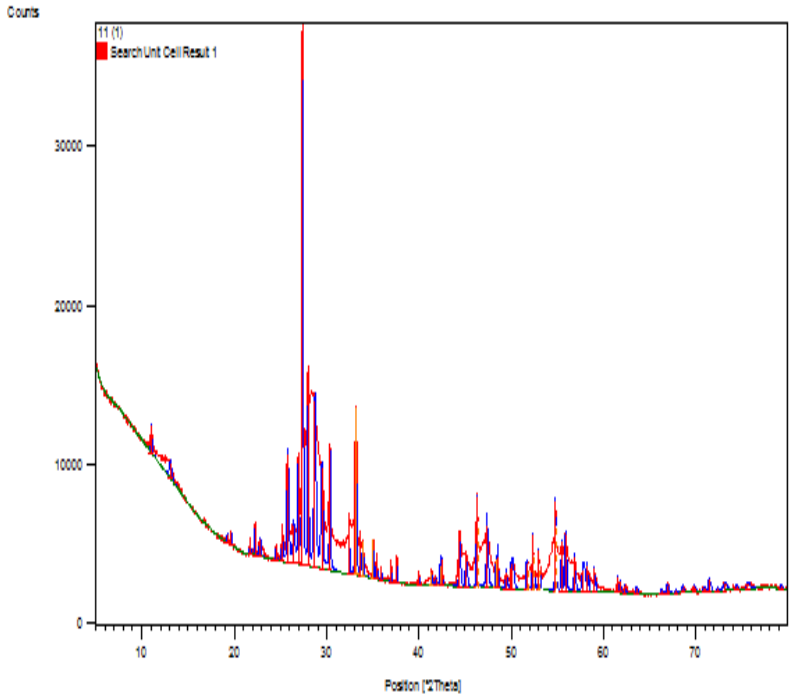

Figure1 Powder XRD spectra of **$Bi_{2.5}$ $Co_{0.25}$ $La_{1.75}$ $N_{0.21}$ O $_{0.25}$ Cl_5**

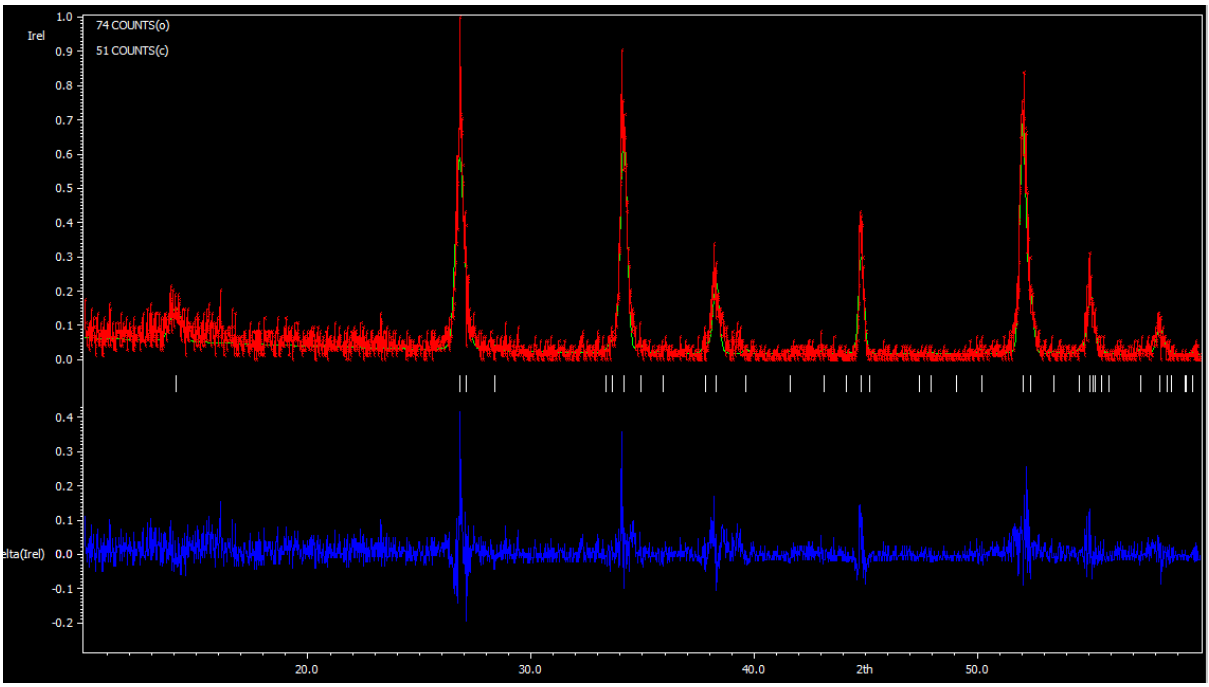

Fig. 2. Graphical representation of the result from Rietveld refinement with X-ray powder data. Vertical bars indicate positions of the Bragg reflections for $\mathbf{Bi_{2.5}\ Co_{0.25}\ La_{1.75}\ N_{0.21}\ O\ _{0.25}\ Cl_5}$ was dots mark the observed intensities and the solid line gives the calculated intensity curve. The deviations between the observed and the calculated intensities from the refined model are shown by the difference plot in the lower part of the diagram.

Reitveld Refinement

The framework structure of $\mathbf{Bi_{2.5}\ Co_{0.25}\ La_{1.75}\ N_{0.21}\ O\ _{0.25}\ Cl_5}$ was first examined by ab initio structure determination method using the powder XRD data. The initial lattice parameters were determined as a=4.214(7) Å b=7.593(11) Å c=13.051(18) Å α=82.22(8)° β=89.97(6)° γ=77.09(8)°° by an indexing procedure using the program TREOR15 in EXPO2004.16 The most probable space group was suggested to be P-1 triclinic crystal system Next, the integrated intensities were extracted by the Le Bail method using the program Jana2006.14 A profile function and background function of the Le Bail method used in the present study were pseudo-Voigt function and 20thorder Legendre function, respectively. An initial structure model was then obtained by the charge flipping (CF) method17 using the extracted integrated intensities. Although the Mn site could not be clearly determined by the CFThe iteration converged with an R factor of 29% and the final electron density shows a P1 symmetry with a 5% error. The program of EDMA was then used to automatically assign atomic positions. Four unique heavy atomic positions were found and the heaviest one was assigned as Bi while the others were considered as Mn and Mo. Due to the existence of heavy atoms, all oxygen positions were ambiguous in the electron density map of this stage[24]. To locate the oxygen atoms, a Monte-Carlo based simulated annealing process with the program TOPAS was applied. For each annealing process, various atomic coordinates were randomly assigned as the initial positions of the oxygen atoms [25]. The annealing process was restarted after finding a few oxygen positions, until all oxygen positions were found to be reasonable.After refinement the possible structure shown in figure 3 and crystallographic data shown in table 1.and fraction coordinate shown in table to which determine the proper position of contained atoms in synthesized compound with mixed valence and refine factors are . Rwp = 0.57.15, Rp = 0.5068 and GOF=0.00178 The structure factors F0 = 3032 and Fc = 3031.

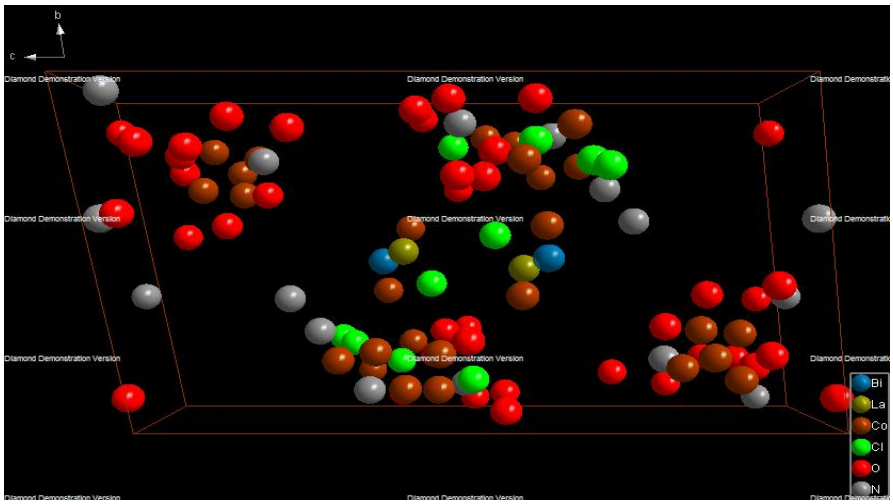

Figure 3 Aurivillius type structure of $Bi_{2.5}\ Co_{0.25}\ La_{1.75}\ N_{0.21}\ Cl_5\ O_{0.25}$

Table 1. Crytallographic Data

Phase data	
Formula sum	**$Bi_{2.5}\ Co_{0.25}\ La_{1.75}\ N_{0.21}\ Cl_5\ O_{0.25}$**
Formula weight	964.5 g/mol
Crystal system	triclinic
Space-group	P -1 (2)
Cell parameters	a=4.214(7) Å b=7.593(11) Å c=13.051(18) Å α=82.22(8)° β=89.97(6)° γ=77.09(8)°
Cell ratio	a/b=0.5550 b/c=0.5818 c/a=3.0971
Cell volume	403.1(11) $Å^3$
Z	2
Calc. density	7.94593 g/cm^3
Meas. density	7.873492g/cm^3
Pearson code	aP92
Formula type	NOP5Q14R18..
Wyckoff sequence	i46

Table 2. Fraction Atomic parameters

Atom	Ox.	Wyck.	Site	.	x/a	y/b	z/c	U [$Å^2$]
Bi1	+3	2i	1		0.72314	0.50484	0.37779	0.0380
La1	+3	2i	1		0.59048	0.47421	0.41282	0.0380
Co1	+3	2i	1		0.98760	0.22224	0.17423	0.0380
Co2	+3	2i	1		0.80945	0.59798	0.37565	0.0380
Co3	+3	2i	1		0.03981	0.86940	0.39078	0.0380
Co4	+3	2i	1		0.90841	0.39831	0.42520	0.0380
Co5	+3	2i	1		0.95625	0.86686	0.32401	0.0380
Co6	+3	2i	1		0.97616	0.77324	0.39768	0.0380
Co7	+3	2i	1		0.07962	0.76393	0.35759	0.0380
Co8	+3	2i	1		0.76799	0.28375	0.12099	0.0380
Co9	+3	2i	1		0.83909	0.18431	0.21240	0.0380
Co10	+3	2i	1		0.95344	0.15610	0.13858	0.0380
Co11	+3	2i	1		0.12851	0.77217	0.44665	0.0380
Co12	+3	2i	1		0.16719	0.88027	0.43581	0.0380
Co13	+3	2i	1		0.82430	0.29633	0.17945	0.0380
Co14	+3	2i	1		0.16678	0.79350	0.29989	0.0380
Cl1	-1	2i	1		0.84411	0.83095	0.37582	0.0380

Cl2	-1	2i	1	0.56055	0.57301	0.44735	0.0380
Cl3	-1	2i	1	0.18546	0.85121	0.48709	0.0380
Cl4	-1	2i	1	0.92174	0.77375	0.30384	0.0380
Cl5	-1	2i	1	0.98231	0.75667	0.28511	0.0380
O1	-2	2i	1	0.92317	0.42703	0.07097	0.0380
O2	-2	2i	1	0.68306	0.30096	0.22210	0.0380
O3	-2	2i	1	0.00282	0.72869	0.48957	0.0380
N3	-3	2i	1	0.09401	0.04154	0.05808	0.0380
N4	-3	2i	1	0.62512	0.89262	0.47335	0.0380
N5	-3	2i	1	0.20711	0.88447	0.33565	0.0380
N6	-3	2i	1	0.21995	0.38218	0.00450	0.0380
N7	-3	2i	1	0.42318	0.61711	0.23694	0.0380

Table 3.Selected bond angles

Atom1	Atom2	Atom3	Angles
Bi1	La1	Co2	131.383
	La1	Co4	88.307
	La1	Cl2	47.346
Co4	Bi1	La1	35.595
	Cl4	La1	88.411
	Cl4	O2	136.041
	La1	O2	74.649
O14	O7	Cl1	108.001
	O7	Co6	69.066
Co14	Co7	Cl5	72.070
	Co7	N5	81.033
	Co7	Co5	56.326
La12	Cl4	Cl5	20.578
	Cl4	Cl1	66.851
	Cl4	N5	105.999

CRYSTAL STRUCTURE OF $Bi_{2.5}\ Co_{0.25}\ La_{1.75}\ N_{0.21}\ Cl_5\ O_{0.25}$

The framework structure of $Bi_{2.5}\ Co_{0.25}\ La_{1.75}\ N_{0.21}\ Cl_5\ O_{0.25}$ was first examined by ab initio structure determination method using the powder XRD data shown in figure 1. The initial lattice parameters were determined by an indexing procedure using the program TREOR15 in EXPO2004.16 The most probable space group was suggested to be P1 triclinic crystal system Next, the integrated intensities were extracted by the Le Bail method using the program Jana2006.[14]. A profile function and background function of the Le Bail method used in the present study were pseudo-Voigt function and 20thorder Legendre function, respectively. An initial structure model was then obtained by the charge flipping (CF) method17 using the extracted integrated intensities. Although the La site could not be clearly determined by the CF method using the powder XRD data, the framework structure of Bi2.5 $Co_{0.25}\ La_{1.75}\ N_{0.21}\ O_{0.25}\ Cl_5$ was successfully determined with the help of Rietveld refinement. Rietveld refinement of Triclnic crystal system having P-1 space group was found with three dimension structure as follows against XRD data for structural determination proved difficult, due to a combination of preferred orientation of the plate-like crystallites in flat-plate geometry[10].In other words, the extracted peak intensities for multi- phase could be reliable. Note that if the relative intensities differed a lot from the simulated patterns of the known phases, additional manual partitioning of those overlapping peaks would be necessary to get reliable intensities for the unknown phase 1. After considering the multiplicity and Lorentz-polarization correction, the intensities of phase 1 were used for the structure solution as below.

Moreover, the reflection conditions indicated possible space group P-1 . The initial structure model was obtained using a charge flipping algorithm with the program Superflip.8 [26] Random phases were used at the beginning of the charge-flipping interaction, and overlapping peaks were re-partitioned using a histogram match to improve the convergence. The iteration converged with an R factor of 29% and the final electron density shows P-1 symmetry with a 5% error. The program of EDMA was then used to automatically assign atomic positions. Four unique heavy atomic positions were found and the heaviest one was assigned as Bi while the others were considered as Zr and Bi. Due to the existence of heavy atoms, all oxygen positions were ambiguous in the electron density map of this stage. To locate the oxygen atoms, a Monte-Carlo based simulated annealing process with the program TOPAS was applied. For each annealing process, various atomic coordinates were randomly assigned as the initial positions of the oxygen atoms The annealing process was restarted after finding a few oxygen positions, until all oxygen positions were found to be reasonable.

MORPHOLOGY STYDY BY SEM

Figure 3.shows a typical SEM image of the $\mathbf{La_{0.5}.Cd_{0.125}.Zr_{0.125}.S_{.0.76}.O_{\ 0.25}.N_{\ 0.125}}$ sample after ion-exchange experiment. The particle morphology and size remained nearly unchanged after ion-exchange reaction. The average particle size was about 1 μm. The FTIR absorption spectrum of the $\mathbf{La_{0.5}.Cd_{0.125}.Zr_{0.125}.S_{.0.76}.O_{\ 0.25}.N_{\ 0.125}}$ sample confirmed that the present sample did not contain water species such as H_2O, OH^- or H_3O^+ in the structure.

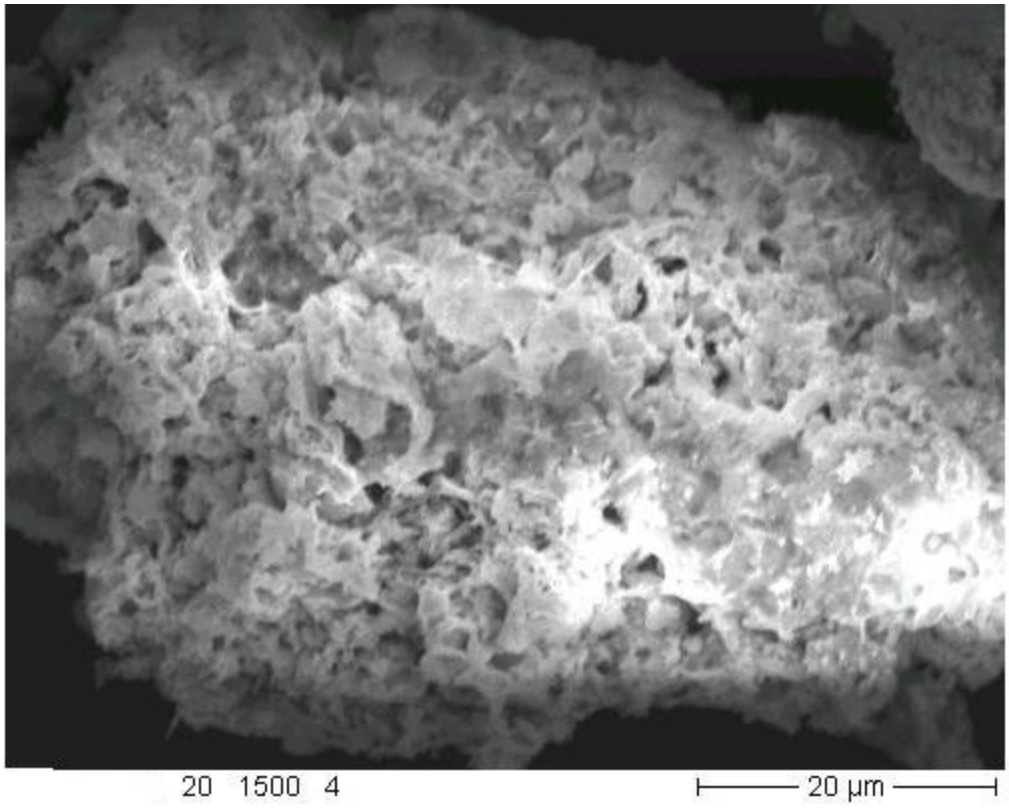

Figure 3. SEM photograph of the Bi2.5 $\mathbf{Co_{0.25}La_{1.75}N_{0.21}O_{\ 0.25}Cl_5}$

DIELECTRIC CONSTANT MEASUREMENT OF Bi2.5 $\mathbf{Co_{0.25}La_{1.75}N_{0.21}O_{\ 0.25}Cl_5}$

The dielectric constant and the dielectric loss of the 10 mm in diameter pellet have been used for the determination of dielectric properties of silver oxide nanoparticles. The corresponding thickness of the pellet was 1.20 mm was studied at different temperature using a HIOKI 3532-50 LCR HITESTER in the frequency range of 50 Hz to 5 MHz. The results of the dielectric constant and dielectric loss as a function of frequency have been plotted in Figs. 6&7. It can be easily interpreted from the plots that the silver oxide nanoparticles show same trend, as having high values of dielectric constant and dielectric loss at low frequencies and decrease with the increase in frequency while reaching to a constant saturated value at high frequencies, depicting a frequency independent behavior. These defects activate interfacial polarizations at low frequencies. Due to this polarization, the dielectric constant is higher at low frequencies. The net polarization of silver oxide is owing to

ionic, electronic, dipolar and space charge polarizations The huge value of the dielectric constant is due to the fact that silver oxide acts as a nanodipole under electric fields [27]. The small-sized particles require a large number of particles per unit volume, important in an increase of the dipole moment per unit volume, and a high dielectric constant. The dielectric constant at low frequencies starts from high value and decreases with increase in temperature. As the temperature increases, the dielectric constant values start increasing. The high value of dielectric constant at low temperature credited to space charge polarization whereas at higher temperature and at low frequencies it possibly connected with defect related conduction processes. The variations of dielectric loss of silver oxide nanoparticles of with frequency and temperature are shown in Fig.8. It can be seen that dielectric loss decreases with increase of frequency and at higher frequencies the loss angle has almost the same value at all temperatures. In dielectric materials, generally dielectric losses take place due to absorption current. The orientation of molecules along the direction of the applied electric field in polar dielectrics requires a part of electric energy to overcome the forces of internal friction one more part of electric energy is utilized for rotations of dipolar molecules and other kinds of molecular transfer from one position to another, which also involve energy losses. In nanophase materials, in homogeneities similar to defects and space charge formation in the inter phase layers create an absorption current ensuing in a dielectric loss[28] As expected, the electrical conductivity of Bi2.5 $\mathbf{Co_{0.25}\ La_{1.75}\ N_{0.21}\ O_{0.25}\ Cl_5}$ measured on sintered powder decreases with increasing temperature, characteristic of multi- metallic behavior.

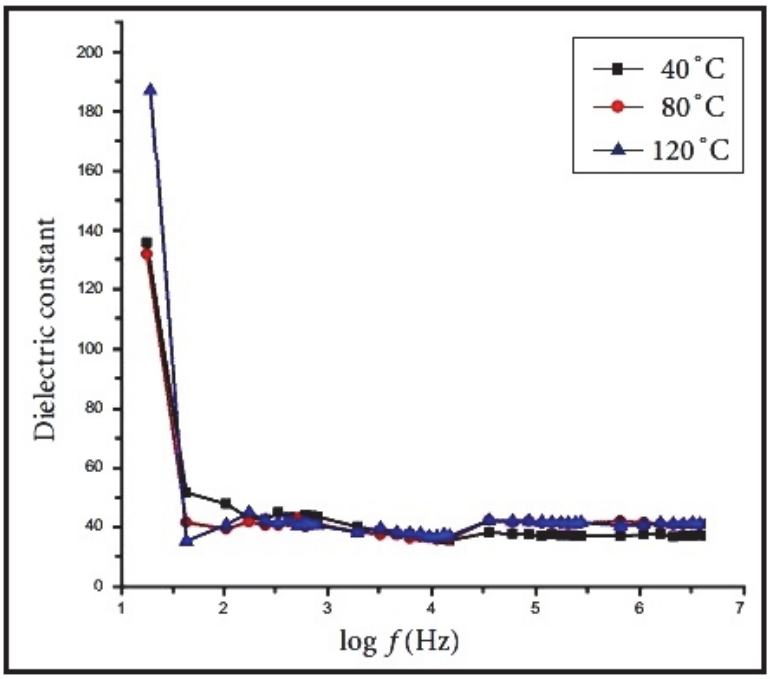

Figure 8...: Dielectric constant as a function of log frequency

The titled metal oxide show nanopartice according to particle size which are placed in the heater and their response is taken at different temperatures[29]. Temperature dependent dielectric constant and dielectric loss has been plotted in Figs. 8 and 9. It is also observed that as the temperature increases, the dielectric constant also increases to a considerable value as seen in Figure. 8. The same trend is observed behavior of dielectric properties with temperature is different over different temperature ranges i.e. at low and high temperature. It is evident from the Fig.6 and 7 that the dielectric constant and dielectric loss are low at a certain room temperature range and remain independent of temperature changes. In high temperature range the dielectric properties rise suddenly and reach a maximum value. The basic reason of the independency of dielectric constant in low temperature range is that impurities remain localized in this range and so conduction is not easy while at high temperature impurities are no more localized and hence conductivity of the material is increased. In case of ionic solids, electrons of the material also become free and contribute to conduction. This results in high polarization of the material; hence value of dielectric constant is increased with increase in temperature. At low and room temperature range, the effect of grain boundaries is dominant and that is why the dielectric properties have small magnitudes and are constant. As the temperature is increased, the role of grains becomes more and more effective and increases in the dielectric properties

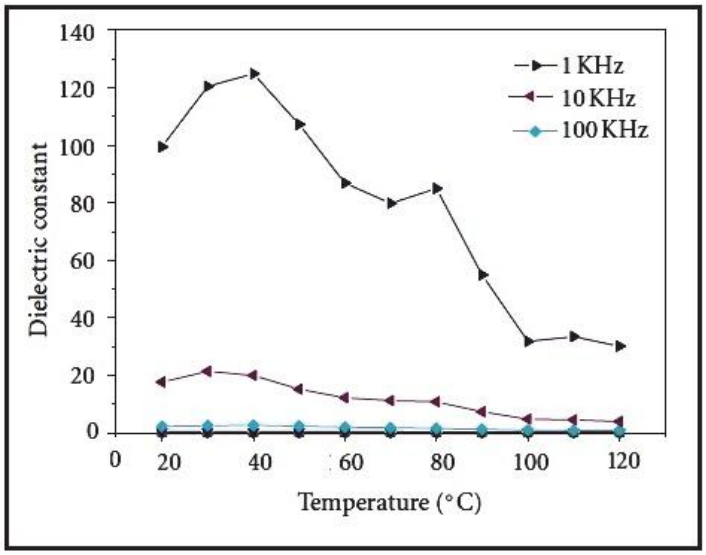

Figure.9.: Temperature dependent dielectric constant of $\mathbf{La_8\ Zr_{28}\ O_{48}\ N_{32}\ Bi_{10}}$

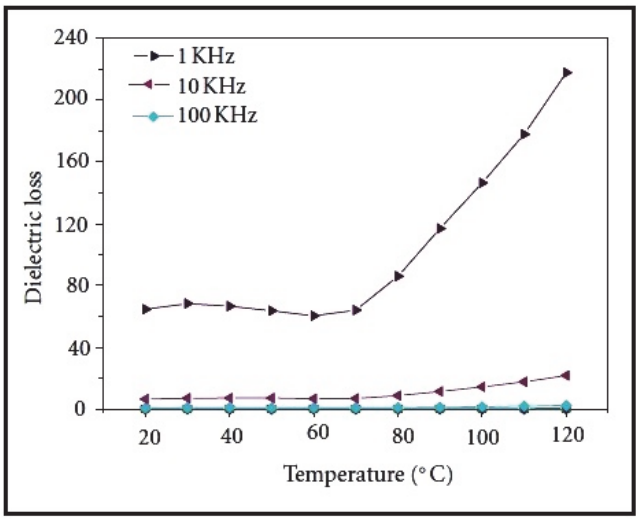

Figure10. Dielectric loss versus temperature

Due to the thermionic emission and tunneling of charge carriers across the barrier, the conductivity increases with the temperature. Because of small size of the particles, the charge carriers reach the surface of the particles more and easily enabling the electron transfer by thermionic emission or tunneling to enhance the conductivity in figure [9.10]. The a.c. conductivities strongly depend on the particle size, the concentration and heat treatment of the sample and the permeating of the electrolytes. Also, the frequency dependent data indicated that the

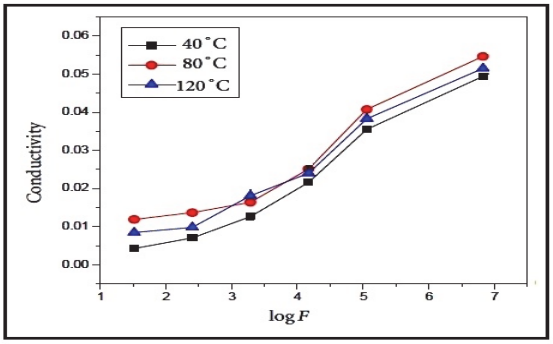

Fig.11. Variation of conductivity with log f

enhancement was due to grains rather than grain boundary or surface conduction. The nature of frequency and temperature dependence of a.c. conductivity of the present samples, suggests an electronic hopping

mechanism[28], exhibited by a large number of nanocrystalline materials. This hopping mechanism is compatible with the highly order and crystal structure of the grain boundary layers of nanophase materials, having high densities of localized levels. This polarization, which is out of phase with the applied electric field, is measured as a.c. conductivity.

IV. CONCLUSIONS

In summary, it may be stated that the room temperature crystal structures of three $n = 4$ Aurivillius type of oxides have been refined from high resolution X-ray diffraction data. The pattern decomposition and peak extraction methods have been used for the first time to derive starting models for $\mathbf{Bi_{2.5}\ Co_{0.25}\ La_{1.75}\ N_{0.21}\ O_{0.25}\ Cl_5}$. A model has been proposed for this high temperature phase. It is also confirmed that the ferroelectric to paraelectric phase transition in $\mathbf{Bi_{2.5}\ Co_{0.25}\ La_{1.75}\ N_{0.21}\ O_{0.25}\ Cl_5}$ is not accompanied by a structural multi -phase transition. The zigzag arrangement of the distorted $\mathbf{Bi_{2.5}\ Co_{0.25}\ La_{1.75}\ N_{0.21}\ O_{0.25}\ Cl_5}$octahedra as observed in the $n = 2$ series of Aurivillius phases are found in these structures as well. A rational explanation for the distribution of the Bi/Co/La cations in the A sites as well as the [Bi2O2]2+ sites is provided based on the VBS calculations. $\mathbf{Bi_{2.5}\ Co_{0.25}\ La_{1.75}\ N_{0.21}\ O_{0.25}\ Cl_5}$ shows a structural transition to the prototype tetragonal structure in the space group *P-1* at 803 K. A model has been proposed for this high temperature phase. It is also confirmed that the ferroelectric to paraelectric phase transition in $\mathbf{Bi_{2.5}\ Co_{0.25}\ La_{1.75}\ N_{0.21}\ O_{0.25}\ Cl_{5\ is}}$ accompanied by a structural phase transition. In other words we can state that the titled mixed valences have been successfully synthesized using stoichiometry chemical technique. X-ray diffraction analysis reveals that the crystallite size of the oxide \particles was found to be 18.32 nm. Spherical shapes morphology of the prepared mixed valence metal oxide was observed in the SEM studies. The transmission electron microscopic analysis confirms the prepared $\mathbf{Bi_{2.5}\ Co_{0.25}\ La_{1.75}\ N_{0.21}\ O_{0.25}\ Cl_5}$ with the particle size of around18.32 nm. Absorption spectrum revealed that the extended absorption wavelength towards the visible-light region. The value of band gap energy obtained from UV absorption spectrum is 570 eV, which was also attributed to the formation of nanocrystalline particles. The variation of dielectric constant, dielectric loss with frequency and temperature for $\mathbf{Bi_{2.5}\ Co_{0.25}\ La_{1.75}\ N_{0.21}\ O_{0.25}\ Cl_5}$ nanoparticles were analyzed. In addition, the plasma energy of the valence electron, Penn gap or average energy gap, the Fermi energy and electronic polarizability of the $\mathbf{Bi_{2.5}\ Co_{0.25}\ La_{1.75}\ N_{0.21}\ O_{0.25}\ Cl_5}$ nanoparticles have been also determined. AC electrical conductivity was found to increase with an increase in the temperatures and frequency. The structure was demined by powder XRD using Rietveld refinement. This oxide will be shown as semi- conductivity character. The ac conductivity plot of the pelletized form of $\mathbf{Bi_{2.5}\ Co_{0.25}\ La_{1.75}\ N_{0.21}\ O_{0.25}\ Cl_5}$nanoparticles is shown in Fig6 .It is observed from the results that the ac conductivity increases with the increase in temperature, which shows the semiconducting nature of the $\mathbf{Bi_{2.5}\ Co_{0.25}\ La_{1.75}\ N_{0.21}\ O_{0.25}\ Cl_5}$.

REFERENCES

[1]. Manickam Minakshi, *ab David R. G. Mitchell,c Christian Baur, b Johann Chable,b Anders J. Barlow, d Maximilian Fichtner,*b Amitava Banerjee,e Sudip Chakraborty e and Rajeev Ahuja,Synthesis of nano particle of mied oide , Nanoscale Adv., 2019, 1, 565

[2]. J. You, L. Xin, X. Yu, X. Zhou and Y. Liu, Synthesis of homogenous CaMoO4 microspheres with nanopits for high-caapcity anode material 詴 Li-ion battery, Appl. Phys. A: Mater. Sci. Process., 2018, 124, 271. 580

[3]. Y. Liang, X. Han, Z. Yi, W. Tang, L. Zhou, J. Sun, S. Yang and Y. Zhou, Synthesis, characterization and lithiumintercalation properties of rod-like CaMoO4 nanocrystals,J. Solid State Electrochem., 2007, 11, 1127–1131.

[4]. Parashuram Mishra, Synthesis, crystal structure determination and ionic properties of novel BiCa0.5Mg0.5 O2.5 via X- ray powder diffraction data Crystal Growth. 2041 32 (2011) 2041-204

[5]. Philipp Bertocco1 · Christoph Bolli1 · Bruno A. Correia Bicho1 · Carsten Jenne1 · Marc C. Nierstenhöfer1 Journal of Chemical Crystallography https://doi.org/10.1007/s10870-019-00773-mah Jebli1 · Abdessalem Badri1 · Mongi Ben Amara1 Journal of Chemical Crystallography https://doi.org/10.1007/s10870-019-00788-3

[6]. N. Tancret, S. Obbade, N. Bettahar,1 and F. Abraha journal of solid state chemistry 124, 309–318 (1996)

[7]. T. Dan Vu,† Firas Krichen,† Maud Barre,† Sandrine Coste,† Alain Jouanneaux,† Emmanuelle Suard,§Andrew Fitch,‖ and François Goutenoire DOI: 10.1021/acs.cgd.8b01552

[8]. Florian, P.; Massiot, D.; Suard, E.; Goutenoire, F. La10W2O21: An Anion-Deficient Fluorite-Related Superstructure with Oxide Ion Conduction. Inorg. Chem. 2014, 53, 147−159.

[9]. Lopez-Vergara, A.; Porras-Vazquez, J. M.; Infantes-Molina, A.; Canales -Vazquez, J.; 11.Cabeza, A.; Losilla, E. R.; Marero-Lopez, D. Effect of Preparation Conditions on the Polymorphism and Transport Properties of La6−xMoO12−δ ($0 \le x \le 0.8$). Chem. Mater. 2017, 29,6966−6975.

[10]. Dubois, F.; Goutenoire, F.; Laligant, Y.; Suard, E.; Lacorre, P. Ab-Initio Determination of La2Mo4O15 Crystal Structure from X-rays and Neutron Powder Diffraction. J. Solid State Chem. 2001, 159, 228−233.

[11]. Thomas E. Weiricha,, Joaquim Portillob,c, Gerhard Coxd,Hartmut Hibste, Stavros Nicolopoulosb,f Ultramicroscopy 106 (2006) 164–175

[12]. A.P. Zhukhlistov, M.S. Nickolsky, B.B. Zvyagin, A.S. Avilov,A.K. Kulygin, S. Nicolopoulos, R. Ochs, Z. Kristallographie 219 (2004) 224.

[13]. [2] D.O. Charkin, Modular approach as applied to the description, prediction, and targeted synthesis of bismuth oxohalides with layered structures, Russ. J. Inorg. Chem. Suppl. 53 (2008) 1977–1996, https://doi.org/10.1134/ S0036023608130019.

[14]. G. Kresse, D. Joubert, From ultrasoft pseudopotentials to the projector augmentedwave method, Phys. Rev. B 59 (1999) 1758–1775, https://doi.org/10.1103/ PhysRevB.59.1758

[15]. Parashuram Mishra, AB Initio Structure Determination of Bi0.5 Mn0.125 Mo0.5 O0.67 U0.32 Mixed Valency From Quartenary of Bi2O3-V2O5 -UO2- Mn2 O2- MoO4, International Refereed Journal of Engineering and Science (IRJES) ISSN (Online) 2319-183X, (Print) 2319-1821 Volume 9, Issue 3 (March 2020), PP. 18-24.
[16]. Bimal K.Kanth and Parashuram Mishra, Synthesis and the Study of Triclinic Crystal Structure a Novel Quaternary Bi0.245 Pb2.351 U1.25 Zr0.8 O4.5 Oxide Contained Mixed Valence by Ab Initio Method via Powder XRD, International Refereed Journal of Engineering and Science (IRJES) ISSN (Online) 2319-183X, (Print) 2319-1821 Volume 9, Issue 3 (March 2020), PP. 41-48.
[17]. Rohit k.dev and Parashuram mishra,Synthesis and ab initio study of crystal chemistry of a novel mixed valence cubical structure of na24bi4cs8 cl26 via powder xrd methodgsj: volume 8, issue 9, September 2020.
[18]. N. Tancret, S. Obbade, N. Bettahar,1 and F. Abraha journal of solid state chemistry 124, 309–318 (1996)
[19]. T. Dan Vu, FirasKrichen, Maud Barre, Sandrine Coste, Alain Jouanneaux, Emmanuelle Suard,Andrew Fitch, and FrançoisGoutenoire Ab Initio structure determination of ternatinary metal oxideDOI: 10.1021/acs.cgd.8b01552
[20]. Florian, P.; Massiot, D.; Suard, E.; Goutenoire, F. La10W2O21: An Anion-Deficient Fluorite-Related Superstructure with Oxide Ion Conduction. Inorg.Chem. 2014, 53, 147−159.
[21]. Lopez-Vergara, A.; Porras-Vazquez, J. M.; Infantes-Molina, A.; Canales -Vazquez, J.; 23..Cabeza, A.; Losilla, E. R.; Marero-Lopez, D. Effect of Preparation Conditions on the Polymorphism and Transport Properties of La6−xMoO12−δ ($0 \leq x \leq 0.8$). Chem. Mater. 2017, 29,6966−6975.
[22]. Dubois, F.; Goutenoire, F.; Laligant, Y.; Suard, E.; Lacorre, P. Ab-Initio Determination of La2Mo4O15 Crystal Structure from X-rays and Neutron Powder Diffraction. J. Solid State Chem. 2001, 159, 228−233.
[23]. Thomas E. Weiricha,,JoaquimPortillob,c, Gerhard Coxd,HartmutHibste, Stavros Nicolopoulosb,Ultramicroscopy 106 (2006) 164–175
[24]. A.P. Zhukhlistov, M.S. Nickolsky, B.B. Zvyagin, A.S. Avilov,A.K. Kulygin, S. Nicolopoulos, R. Ochs, Z. Crystal structure of metal oxideKristallographie 219 (2004) 224.
[25]. [2] D.O. Charkin, Modular approach as applied to the description, prediction, and targeted synthesis of bismuth oxohalides with layered structures, Russ. J. Inorg. Chem. Suppl. 53 (2008) 1977–1996, https://doi.org/10.1134/S0036023608130019.
[26]. G. Kresse, D. Joubert, Fromultrasoftpseudopotentials to the projector augmentedwave method, Phys. Rev. B 59 (1999) 1758–1775, https://doi.org/10.1103/ PhysRevB.5

Janak Adhikari, et. al. "Synthesis, Structure Determination and Study the Electrical Properties of A Novelmixed Valence of Bi2.5 Co0.25 La1.75 N0.21 Cl5 O 0.25 Chloro Oxide by AB Initio Methods VIA Powder XRD." *International Journal of Engineering and Science*, vol. 10, no. 12, 2020, pp. 18-27.